NOTES ON SCALING AND CRITICAL BEHAVIOUR IN NUCLEAR FRAGMENTATION

X. Campi and H. Krivine

Division de Physique Théorique [1]
Institut de Physique Nucléaire
F-91406 Orsay Cedex, France

Contribution to the V La Rábida
International Summer School.
June 1994
La Rábida (Spain).

To be published by Springer Verlag

IPNO/TH 94-83

[1] Unité de Recherche des Universités Paris XI et Paris VI associée au CNRS.

NOTES ON SCALING AND CRITICAL BEHAVIOUR IN NUCLEAR FRAGMENTATION

X. Campi and H. Krivine

Division de Physique Théorique[1]
Institut de Physique Nucléaire
91406- Orsay Cedex, France

Abstract. We discuss the relevance of the concepts of scaling and critical behaviour in nuclear fragmentation. Experimental results are reviewed to check whether the signals of a percolation or liquid-gas phase transition manifest themselves in the data.

Keywords. Multifragmentation, Phase Transitions, Percolation

1 Introduction

Excited nuclei decay according to various deexcitation modes. At energies up to a few MeV/*nucleon*, the main mode is light particle emission. At energies of the order of five to ten MeV/nucleon, this mode is relayed by the emission of medium mass fragments (see Fig. 1). The aim of these lectures is to discuss this nuclear fragmentation in the general framework of modern theories of fragmentation. The study of this new and fast developing field of statistical mechanics, concerns many physical systems of the microscopic world, including polymers, gels, atomic clusters, nuclei and elementary particles. One of the goals of this research is to investigate what are the features that are common to various fragmentation processes, regardless the nature of the elementary constituents or the binding interactions of the fragmenting objects. A particularly significant outcome of this research is the realization that in many circumstances the fragment size distribution (FSD) is scale invariant. Another realization is that quantities associated to the FSD can show a critical behaviour, i.e. can diverge at some critical points. These realizations clear the way to a model independent classification of the various fragmentation mechanisms in terms of the scaling properties and critical behaviour. Applying these concepts to nuclear fragmentation would

[1] Unité de Recherche des Universités de Paris 11 et Paris 6 associée au CNRS

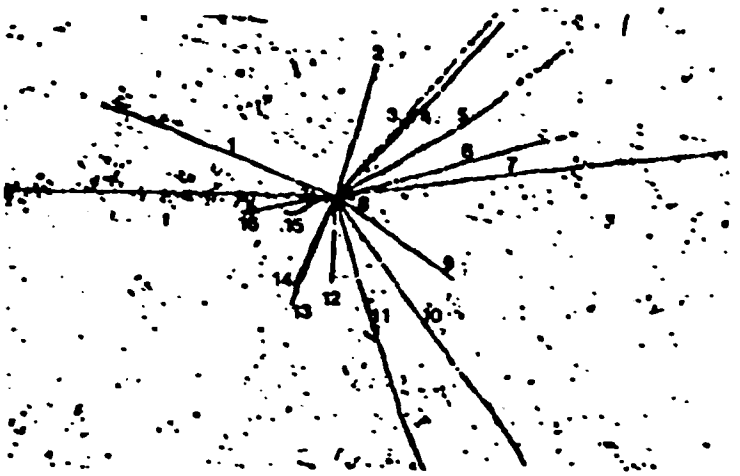

Figure 1: *The collision of a 850 MeV ^{12}C projectile arriving from the left with an Ag (Br) target in a nuclear emulsion. The charge $1 \leq z_i \leq 4$ of 16 fragments has been identified. From Ref. [1].*

be very fruitful. It would clarify what features are generic, (for example common to all finite size systems with short range attractive forces) and what features are specific of nuclei (for example, what is the influence of quantum effects, of the combination of a short range attraction with a long range coulomb repulsion, of the presence of two types of particles, etc.).

The presence of this critical behaviour in the FSD can be the manifestation of a phase transition in nuclear matter. One of the present goals of heavy ion physics is the determination of the equation of state of infinite nuclear matter. The knowledge of this object in a wide range of physical conditions is fundamental for future developments of nuclear theory as well as a basic input for astrophysics. Particularly interesting is the behaviour of the equation of state in the vicinity of phase transitions. For example, one expects [2] that at a temperature of about 6 to 10 MeV takes place in infinite nuclear matter a sort of liquid-gas phase transition. We ignore if it is possible to study this phase transition in the laboratory. By energetic heavy ions collisions we are able to produce during short times very small pieces of nuclear matter at the required conditions, but we dont know what are the signals of a "phase transition" in a transient state of a so small system. In this notes we will discuss how to approach this problem. The reader may find it useful to consult review papers that emphasize different and complementary aspects of nuclear fragmentation [3, 4, 5].

These notes are organized as follows. In Section 2 we give a brief report on models of fragmentation, with emphasis on practical realizations in nuclear

m	n_s
6	6 0 0 0 0 0
5	4 1 0 0 0 0
4	3 0 1 0 0 0
4	2 2 0 0 0 0
3	2 0 0 1 0 0
3	1 1 1 0 0 0
3	0 3 0 0 0 0
2	1 0 0 0 1 0
2	0 1 0 1 0 0
2	0 0 2 0 0 0
1	0 0 0 0 0 1

Table 1: *Partitions of $S = 6$ according to the multiplicity m. The rows indicate the values of n_s.*

physics. Section 3 is devoted to develop the concepts of scaling and critical behaviour. In Section 4 we discuss how this concepts would apply to nuclear fragmentation. Some final remarks are made in Section 5.

2 Elements of theory

A theory *ab initio* of fragmentation, i.e. starting for instance from the Schrödinger equation, is of course not available. In fact such theory would be probably useless. On the other hand, it is dubious that a unique theory explaining the fragmentation of all kinds of clusters (nuclear, atomic, molecular, macroscopic...) can be constructed. The statistics obeying the constituents (fermions or bosons), their size and their interaction (shape, intensity and range) may play crucial roles. In this section we will describe a few very simple fragmentation models that make abstraction of all these (important ?) details. In contrast, we put the emphasis on global properties, like scaling, that would be universal for certain classes of fragmentation.

2.1 Partitions

A partition by definition is a collection of integers (with given sum) without regard to order. The integers collected to form a partition are called its parts, and the number which is the sum of these parts is the partitioned number. It is conventional to abbreviate repeated parts by use of a multiplicity vector.

We will use the following notations : S will be the size (mass or charge) of the nucleus that is partitioned, s the size of its parts (fragments), which appear

with multiplicity n_s. For example the 11 partitions of number 6 are displayed in Table1. Let also be s_{max} the size of the largest fragment. Constituents number conservation is expressed through the multiplicities n_s by

$$S = \sum_{s=1,s_{max}} s n_s. \tag{1}$$

With any given partition one can associate its parts (fragments) multiplicity m, defined as

$$m = \sum_{s=1,s_{max}} n_s. \tag{2}$$

The number $N(S,m)$ of partitions having multiplicity m is calculated by the recurrent relation

$$N(S,m) = \sum_{0 \le k \le (S/m)-1} N(S-km-1, m-1).$$

The *total number of partitions*

$$N(S) = \sum_{m=1,S} N(S,m)$$

grows very rapidly with S. For large S this number can be estimated by[6]

$$N(S) \simeq \frac{e^{\pi\sqrt{2/3S}}}{4\sqrt{3}S}. \tag{3}$$

For example, $N(100) = 190569292$ while formula 3 gives $19.9.10^7$.

The basic quantity in a fragmentation process is the probability $P\{n_s\}$ to observe a partition $\{n_1, \cdots, n_S\}$. This probability may be governed by conservation laws, by geometrical constraints, by *equilibrium* (thermal, chemical, statistical...) conditions, etc.

Assuming that the probability p_s of emitting a fragment of mass s is independent of how the rest of the nucleus disintegrates, the probability of observing a partition of multiplicity m is given by the multinomial distribution

$$P(n_1.....n_S) = \frac{p_1^{n_1} p_2^{n_2} \cdots p_S^{n_S}}{n_1! n_2! \cdots n_s!} m! \tag{4}$$

restricted by $\sum_s s n_s = S$. Because of the very large number of partitions, this hypothesis can only be checked in detail for small systems. Cole and collaborators [7] have studied the fragmentation of carbon nuclei ($S = 12$, 57 different partitions). Taking p_s from the experimental inclusive mass distribution σ_s (all fragmentation events)

$$p_s = \frac{\sigma_s}{\sum_s \sigma_s},$$

they found that Eq. 4 accounts for data better than a factor of two for most partitions. The largest deviations are observed in partitions for which typical nuclear physics effects are strongest (for example the decay in three α particles).

To begin with a study of fragmentation we do not need all the information carried by $P\{n_s\}$. The average fragment size distribution of partitions of a given type suffices, in a first step, to characterize the models and the data. In what follows, we denote this average by n_s. We turn now to the description of various fragmentation models of increasing complexity.

2.1.1 Maximum Entropy

A natural starting point, when no a priori information on the fragmentation mechanism is known, is to make the hypothesis that all partitions of a given type are equally probable. This is called the "Maximum Entropy" principle. Assuming that only the mass (or charge) S is conserved, Aichelin et al. [8] derived the asymptotic expression

$$n_s \simeq \frac{1}{e^{(1.28s/\sqrt{S})} - 1}.$$

One of the shortcomings of this approach is the lack of a control parameter associated to the "violence" of the fragmentation. Moretto and Bowman [9] have added the constraint of a given total surface of the fragments. The idea is that the excitation energy is proportional to the extra surface created by the formation of fragments. The FSD is then

$$n_s = \frac{1}{e^{Ds + As^{2/3}} - 1}. \tag{5}$$

The coefficients A and D are obtained by solving the equations

$$S = \sum_s \frac{a}{e^{Ds + As^{2/3}} - 1},$$

$$Surf = k \sum_s \frac{a^{2/3}}{e^{Ds + As^{2/3}} - 1},$$

where $Surf$ is the surface produced and $k = 3^{2/3}$ for spherical shapes. In order to confront Eq. 5 with data, it remains to convert this surface production in excitation energy.

Notice that, in all circumstances, these FSD are exponentially decaying. We will see below that for a critical phenomenon one expects a power law decay.

2.1.2 Geometrical Models

These models consist in ensembles of points in a *space*, which are *linked* by some mechanisms. The points represent the positions of the constituents in the space (coordinate, phase space...). The positions of the points are either fixed (static models) or change with time (kinetic models). The linkage mechanisms are in general very simple *random* mechanisms based on *proximity* rules. Remark that "geometrical" is used here in a very loose sense. We will describe percolation models in some details with the purpose to introduce critical phenomena and finite size scaling manifestations in cluster production.

A percolation model is a collection of *static* points (sites) distributed in space, certain pairs of which are said to be adjacent or linked [11]. Whether or not two sites are linked is governed by a *random* mechanism the details of which depend on the context in which the model is used. There are two main classes of percolation known as bond and site percolation. In the site problem, the sites are occupied at random with a probability p. All bonds between occupied sites located at less than a certain distance are active. In the bond problem, all sites are occupied and bonds are active with probability p. The sites may be partitioned into *clusters* such that pairs of occupied sites in the same cluster are connected by active bonds. There is no path between sites in different clusters.

When p is close to zero, most sites will be isolated or form very small clusters. In the opposite, if p is close to one then nearly all sites are connected forming *one* large cluster, which occupies most of the available sites (or joins the borders of the system). This is called a "percolation" cluster. It is observed that in sufficiently large systems (see below), there is either one or none, but never two or more such percolation clusters. For infinite systems a sharply defined percolation threshold p_c exists such that for $p < p_c$ no percolating cluster exists and for $p > p_c$ *one* percolating (infinite) cluster exists. The transition from a non-percolating state to a percolating state is a kind of phase transition. The main difference between percolation and other phase transitions is the absence of a Hamiltonian. The percolation transition is a purely *geometrical* phenomenon in which the clusters are clearly defined *static* objects.

For theoretical purposes it is simpler to consider percolation models on a regular lattice. This reduction is done without any loss of generality because the behaviour of the percolation model near the critical point is independent on the details of the lattice. This behaviour is characterized by the *critical exponents*, which are "universal" to all short range linkage models of the same euclidean dimension d. This means, for example, that the exponents for triangular and square lattices ($d = 2$), site or bond percolation, are strictly the same although the percolation thresholds p_c may vary by a factor of two. In percolation theory, the critical exponents are associated to the FSD. The average number of clusters *per lattice site* has been shown [11] to follow approximately a scaling relation near p_c for large cluster sizes s :

$$n_s(\epsilon) \sim s^{-\tau} f(s/s_\xi(\epsilon)) + \cdots \qquad (6)$$

where $\epsilon \sim p - p_c$ and $s_\xi(\epsilon)$ is the characteristic cluster size, that diverges at $p \to p_c$ as

$$s_\xi \sim |\epsilon|^{-1/\sigma} . \tag{7}$$

Here τ and σ are two critical exponents and f a scaling function satisfying $f(0) = 1$, i.e at the critical point $n_s \sim s^{-\tau}$. Remark that τ and σ are "universal" once d is fixed, but f is model dependent.

The size s_{max} of the percolation cluster, that exists only for $p > p_c$, goes to zero as

$$s_{max}/S \sim (p - p_c)^\beta \tag{8}$$

where β is another critical exponent. This quantity plays the role of the *order parameter* in percolation theory (it is null in the most symmetric phase and takes a finite value in the other).

For percolation in $d = 1$ and $d = 2$ dimensions, the exact values of these exponents are known. For $d \geq 6$, the mean field values become exact. For $d = 3$ and 4, only approximate values obtained from Monte Carlo simulations are known.

In Fig. 2 we show the behaviour of n_s for the bond percolation model in a cubic lattice with 4^3 sites. Fig. 1*a* is for $p \ll p_c$ and Fig. 1*d* for $p \gg p_c$. One remarks that in both cases the distribution of light fragments is an exponential-like decreasing function. One also sees in Fig. 1*d* the broad distribution of s_{max} (centered around $s = 55$). At the critical "point" (Fig. 1*b*), the distribution is a power law (remark the change to a log-log representation). For p lightly above this point (Fig. 1c), one sees the rise of the percolation cluster.

The site and bond percolation models considered so far can be combined into a site-bond percolation model. Then the sites are occupied with probability q and the bonds between nearest neighbour occupied sites are active with probability p. As shown in Fig. 3, for any probability q larger than the site percolation threshold, there is a percolation threshold $p_c(q)$ for the bond probability. For $p > p_c(q)$, a percolation cluster exists. There is strong numerical evidence that the whole percolation line is described by the usual percolation exponents.

For pedagogical purposes, we will derive Eq. 6 in one dimension. Consider a linear chain of sites containing L sites. Each of these sites is randomly occupied with probability p (empty with probability $(1 - p)$) and all the bonds between nearest neighbours are active (site percolation model). The probability that s arbitrary sites are occupied is p^s. The probability of one end having an empty neighbour is $(1-p)$ and therefore the total probability to find an $s-$cluster is $p^s(1 - p)^2$. When L is large and $p < 1$, boundary effects are negligible. Then $Lp^s(1 - p)^2$ is the total number of s – clusters, and the number of s – cluster per lattice site is

$$n_s^{sit.}(p) = p^s(1 - p)^2. \tag{9}$$

Analogous reasoning gives for the bond percolation

$$n_s^b(p) = p^{s-1}(1 - p)^2. \tag{10}$$

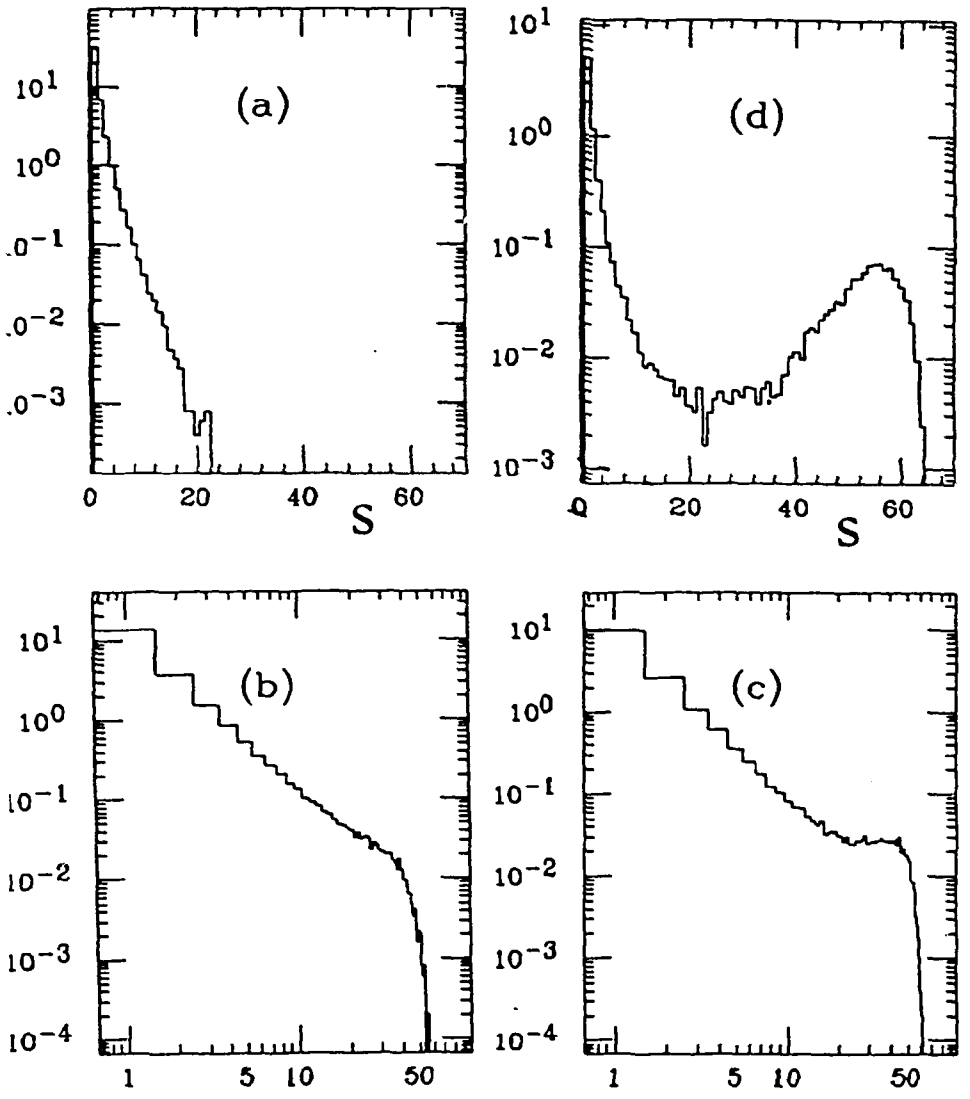

Figure 2: *Fragment size distribution n_s in a percolation model with a cubic lattice containing 4^3 sites : a) $p \ll p_c$, b) $p = p_c$, c) $p \geq p_c$, d) $p \gg p_c$.*

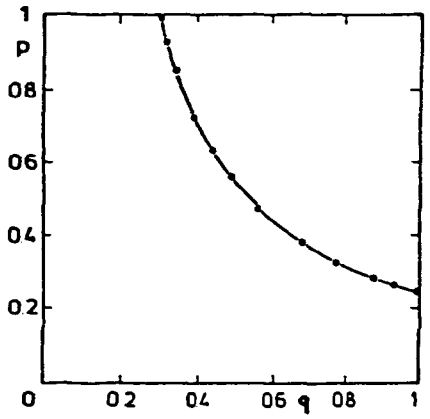

Figure 3: *Phase diagram of site-bond percolation in the cubic lattice. In this lattice the bond percolation threshold is at 0.248 and the site percolation threshold at 0.312. From ref. [10].*

We now discuss the consequences of Eq. 9.

When $p = 1$ all sites are occupied and the chain contains a single infinite cluster called *percolation cluster*. For every value $p < 1$ the chain will have on average $(1 - p)L$ empty sites and there is no percolation cluster. The percolation threshold is at $p = 1$. Because $p \leq 1$, there is no phase transition in this one dimensional model, as usual [12]. Nevertheless we will see that the system approaches a critical behaviour as given by Eq. 6 when $p \rightarrow p_c = 1$. We can write as in Ref. [13]

$$p = e^{\log p} \simeq e^{p-1} = e^{p-p_c},$$

therefore

$$n_s^{sit.}(p) \simeq s^{-2}[(p_c - p)s]^2 e^{-(p_c-p)s} = s^{-\tau} f(s/s_\xi)$$

with $\tau = 2$, $\xi = (p_c - p)^{-\sigma}$, $\sigma = 1$ and $f(z) = z^2 e^{-z}$. Remark that when $p \ll p_c$, n_s decreases exponentially with s (and as a power law when $p \rightarrow p_c$, see Eq. 9).

Cluster size distributions given by Eqs. 9 or 10 may be seen as signatures of fragmentation of 1-dimensional objects. In most practical application is better to work with the moments of n_s,

$$m_k = \sum_s s^k n_s.$$

or by the combination

$$\gamma_2 = \frac{m_2 m_0}{m_1^2} \tag{11}$$

which characterizes the width of the FSD n_s.

For example for 1-dimensional site percolation we have

$$\left.\begin{array}{rcl} m_o &=& 1-p \\ m_1 &=& p \\ m_2 &=& p(1+p)/(1-p) \\ &\vdots& \end{array}\right\}$$

The second moment of the FSD can be rewritten in the form

$$m_2 = p(1+p)(1-p)^{-\gamma}$$

that diverges at threshold with the critical exponent $\gamma = 1$.

The *correlation function* $g(r)$ is defined as the probability that a site a distance r apart from an occupied site belongs to the same cluster. Obviously $g(0) = 1$, $g(1) = p$ and in one dimension,

$$g(r) = p^r = e^{r\,log p}$$

and

$$\log p = \log[1-(1-p)] \simeq p - 1.$$

Therefore

$$g(r) \simeq e^{-\frac{r}{\xi}} \simeq \frac{1-r}{\xi}$$

where

$$\xi = \frac{1}{1-p} \simeq (p_c - p)^{-\nu}$$

is the *correlation length* and $\nu = 1$ another critical exponent.

In summary, in 1-dimension percolation we have the set of critical exponents : $\tau = 2$, $\gamma = 1$, $\nu = 1$ and $\sigma = 1$.

2.1.3 Nuclear Percolation

Percolation ideas have been implemented in various nuclear fragmentation models. The nucleus is idealized by an ensemble of nucleons (sites), linked by the short range nuclear force (bonds). In a cold nucleus, all sites are occupied and all bonds between nearest neighbours are active. During a nuclear collision, the number of active sites decreases (because nucleons are ejected out of the nuclear volume or because the system expands the density decreases), and the number of active bonds also decreases (because the expansion breaks the short range bonds). The bond activation parameter plays the role of an excitation energy and the site parameter the role of the density.

In ref. [14], one uses a one-dimensional bond percolation model in combination with a standard particle evaporation model. Three-dimensional bond percolation in a cubic lattice was examined by Bauer et al. [15], continuous percolation (percolation without a lattice) in ref. [16] and site-bond percolation by Desbois in ref. [17]. Sometimes this model is coupled to a dynamical theory that gives information about the distribution of p and q parameters [18, 19, 20].

2.1.4 Statistical equilibrium

In the theories of cluster fragmentation we have considered so far the weight of the various partitions as given only by combinatorics and geometry. Although these theories are very successful in predicting many global features of data (see Section 4), in some physical situations it is necessary to take into account explicitly energy and momentum conservation. This is the case for example in low bombarding energy fragmentation, where the binding energies of the individual clusters play a dominant role in defining the fragmentation pathway. The simplest way to incorporate this information is to adopt a thermodynamic point of view and say that after a complicated break-up phenomenon the available phase-space is homogeneously filled by the events. Let's be more precise [21]. For a complicated process the transition probability $P_{i\alpha}$ from the initial i to any find state α is mainly constrained by particle number S, energy E and momentum $\vec{P}$ conservation, i.e. $P_{i\alpha}$ is essentially the same for all allowed final states and zero otherwise.

We have

$$P_{i\alpha} = 1/\xi \quad or \quad P_{i\alpha} = 0$$

where

$$\xi = \sum_{\{n_i^\alpha\}} \delta(E - E_\alpha)\delta(S - \Sigma\ n_i^\alpha s_i)\delta^3(\vec{P} - \Sigma\ n_i^\alpha \vec{P}_i) \qquad (12)$$

is the available phase space (the partition function in the microcanonical ensemble) of decay channels. The various decay channels are well defined by specifying the fragments in each channel α, i.e. their number n_i^α their mass s_i, position $\vec{r}_i$, and momentum $\vec{P}_i$.

The channel energy E_α is defined as

$$E_\alpha = \sum_i n_i^\alpha \left(B_i + \frac{P_i^2}{2m_i} + \varepsilon_i^* \right) + C_\alpha$$

where B_i is the binding energy of fragment i, ε_i^* its internal excitation energy and C_α is the Coulomb interaction energy between the fragments. The partition function (Eq. 12) has been calculated in a nuclear context using an infinite matter approach [22], solving a *selfconsistent system of many* (up to 3000) non linear coupled equations or using a Monte-Carlo simulation of possible decay channels putting at random fragments inside a sphere of a fixed volume [23]. Work on similar lines has also been done by the Copenhagen group[24].

This model explicitly incorporates quantum shell effects through the binding B_i and internal excitation energies ε_i^* and the effects of the long range repulsive interactions between the clusters. It shows characteristic phase transitions, one at a temperature of about 5 MeV, which is of fission type and specific of nuclear systems and another at $T \sim 6-7$ MeV of droplets condensation type [25]. The canonical heat capacity, which is the classical observable of a phase transition, clearly shows two peaks at these temperatures (see Fig. 4).

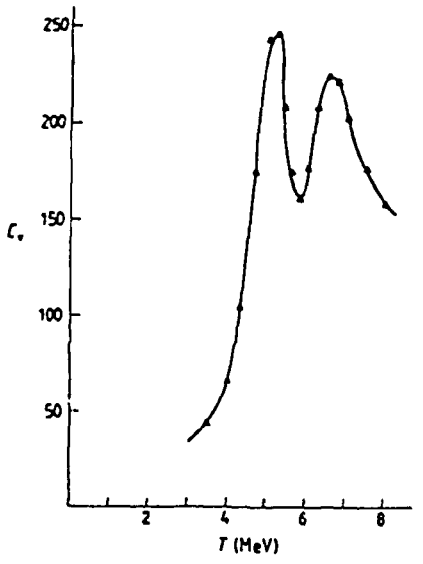

Figure 4: *Canonical heat capacity for* ^{131}Xe *as a function of temperature, calculated with the statistical equilibrium model. From ref. [4]*

2.1.5 Rate Equations Theory

So far we have considered *static* approaches of cluster fragmentation. However in some cases it is important to take into account the time evolution of the fragmentation process.

Assuming that the breakup process is driven by an external source, the time evolution of the fragment-size distributions for systems undergoing fragmentation may be described by a system of *linear* rate equations,

$$\frac{\partial}{\partial t} n_x(t) = -a(x) n_x(t) + \int_x^\infty n_y(t) a(y) f(x \mid y) dy. \tag{13}$$

Here $n_x(y)$ is the number of fragments of size x per unit volume at time t. The first term in the right-hand side represents the loss of particles of size x due to the breaking into smaller ones at a rate $a(x)$. The integral term represents the increase of particles of size x because of the breakup of larger ones. The rate at which x is produced from y is denoted by $f(x \mid y)$. This quantity must be normalised so that mass is conserved

$$\int_0^y x \, f(x \mid y) dx = y.$$

The number of fragments is given by

$$\bar{N}(y) = \int_0^y f(x \mid y)dx.$$

For the particular case of binary breakup, $f(x \mid y) = f(y - x \mid y)$ and $\bar{N} = 2$. Cheng and Redner [26] developed a scaling theory for homogeneous breakup kernels for which

$$a(x) = x^\lambda,$$

where λ is the homogeneity index. Homogeneity also implies that,

$$f(x \mid y) = y^{-1} b(x \mid y). \tag{14}$$

The analysis of Eq. 13 is done with the scaling cluster size distribution given by 6

$$n_y(t) \sim s^{-2}\phi(y/s(t)).$$

Here the typical cluster mass decreases according to Eq. 13 as

$$s(t) \sim t^{-1/\lambda},$$

for $\lambda > 0$. The main results are summarized as follows. For large x, $\phi(x)$ has the universal asymptotic form

$$\phi(x) \sim x^{b(1)-2}e^{-\alpha x^\lambda}, \quad x \to \infty$$

with $b(1) \geq 0$.

For small x, $\phi(x)$ may decay as

$$\phi(x) \sim \exp\left[-\frac{\lambda}{2\ell n x_0}(\ell n^2 x)\right] \quad x \to 0,$$

when it exists a sharp cut off in the kernel at small fragment sizes, i.e. $b(x) = 0$ for $x < x_0$ and $0 < x_0 < 1$. When there is no small size cut off the decays of $\phi(x)$ approaches a power law

$$\phi(x) \sim x^\nu \quad x \to 0.$$

A "shattering" transition takes place when $\lambda < 0$, in which clusters of indefinitely decreasing size are produced. This process is analogous to, but opposite from, the gelation found in aggregation systems.

Exact solutions of Eqs. 13 have also been obtained by Mc Grady and Ziff for analogous rate kernels[27] and for discrete binary breakup models[28].

Some attempt has been made to describe nuclear fragmentation in terms of a sequential-binary decay process. We will mention the realistic calculations of the statistical decay code GEMINI [40] and the semi-analytical model of Richert and collaborators [41].

2.2 Comparison with experimental data

Here we will compare with experimental data some predictions of the previously described models. The models are the following.

a) The sequential-binary decay model, in the GEMINI version [40].

b) The statistical equilibrium model, in the Copenhagen version [38].

c) The site-bond percolation model.

The first and second models, need as input parameters the distributions of excitation energies and the sizes of the breaking systems. These informations have been taken from a *BUU* calculation. For the percolation model [34], the bond probability has been adjusted at $p = 0.45$, while the site occupation probability varies randomly $0 < q < 1$, to mimic the variation of the size of the system with the violence of the collision. The experimental data is from the ALADIN experiment [34]. It concerns the fragmentation of *Au* projectiles bombarding different targets at energies of 600 MeV/nucleon. Event by event, all charged fragments are detected (except those with $z = 1$ and some with $z = 2$). The events are classed according to the variable Z_{bound}, that is the sum of all the detected charges of the event. There should be some anti-correlation between this variable with excitation energy, since small Z_{bound} means large number of (undetected) protons and large excitation energy.

As a function of Z_{bound}, we show in Fig. 5 the following quantities. a) The average charge $< Z_{max} >$ of the largest fragment. b) The average multiplicity of intermediate mass fragments (IMF). c) The average value of the relative asymmetry between the largest and the second largest charges in the event. d) The average width of the fragment size distribution (see Ref. [34] for the exact definition). The symbols are the experimental points. The dashed, dotted and continuous lines are the predictions of the statistical equilibrium, GEMINI and percolation models respectively.

The statistical equilibrium model under the size of the largest fragment at low Z_{bound}. The position of the peak of $< M_{IMF} >$ and $< \gamma_2 >$ is almost correct, but the width of the curves is too small. The relative asymmetry of the largest fragments is underpredicted[2]. The GEMINI model fails in all predictions. In particular, it does show no clear maximum for $< \gamma_2 >$. This is because this model does not have a critical behaviour. The percolation model can describe these data with surprising accuracy, despite their simplicity and their absence of nuclear physics content. This probably means that the observables a)-c) reveal an universal behaviour of a finite size fragmenting system interacting with short range forces and that this behaviour is well represented by percolation theory.

[2]By adjusting as free functions the energy and source size distributions, it is possible to reproduce well the data with a statistical equilibrium model [39], but the adjusted energies are as much as a factor of two smaller than the BUU predictions.

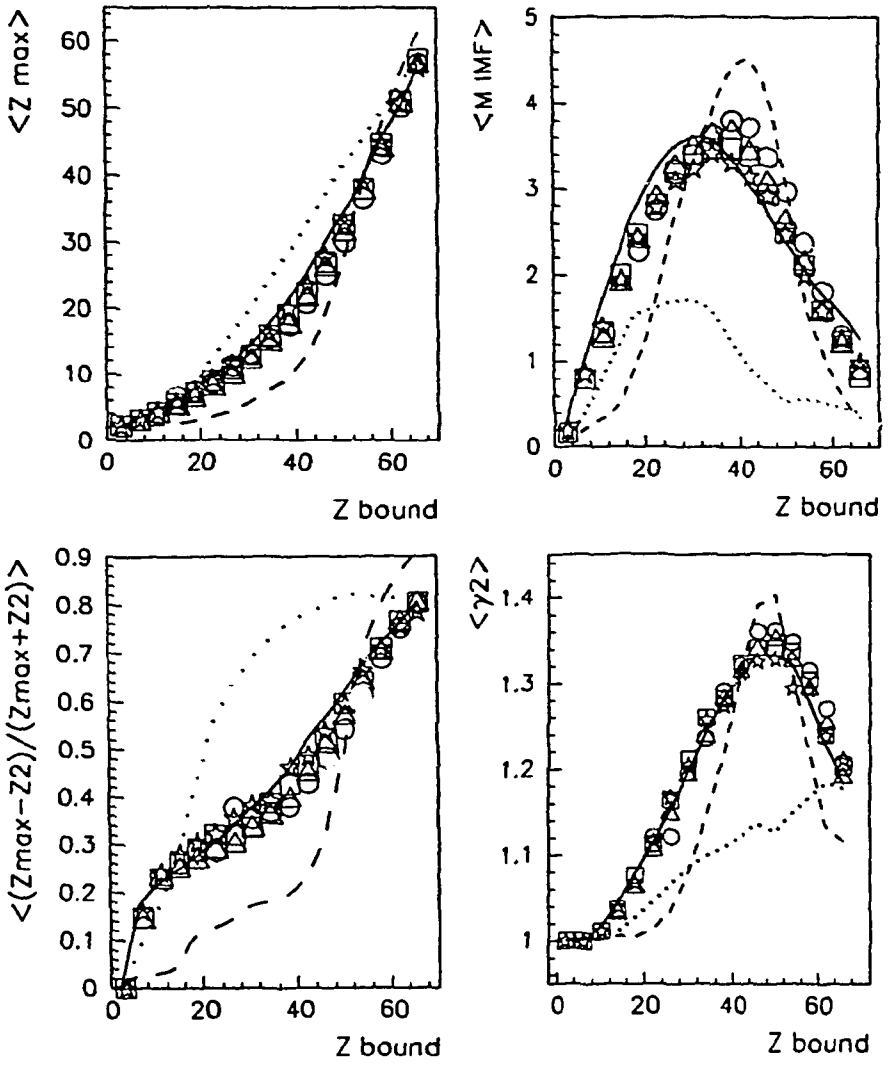

Figure 5: *The average charge* $< Z_{max} >$ *of the largest fragment (a), the mean number of intermediate mass fragments* $< MIMF >$ *(b), the average value of the relative asymmetry for the two largest fragments (c) and the average reduced width of the fragment charge distribution* $< \gamma_2 >$ *as a function of* Z_{bound} *(see text). Experimental data is from ALADIN experiment on Au 600 Mev/nucleon on C (circles), Al (triangles), Cu (squares) and Pb (stars). The lines are the statistical equilibrium (dashed), GEMINI (dotted) and percolation (continuous) predictions.*

3 Scaling and critical behaviour

First we recall some basic definitions concerning critical phenomena. For a detailed discussion, the book of Stanley[29] remains the standard reference in the field.

Let's start with a mathematical introduction of scaling. In physics, many functions $F(x,y)$ of two variables approach to the leading order, if both x and y approach zero, the simpler form

$$F(x,y) = x^A f(y/x^B) \tag{15}$$

where f is a continuous function. (If a variable goes to infinity, use the reciprocal value of this variable). For example, $F(x,y) = (x+\sin(x/y))/(y+xy)$ looks very complicated, but if x and y go to zero with fixed ratio than we get asymptotically $F(x,y) = (x/y)\sin(x/y)/x$. Thus in Eq. 15, $A = -1$ $B = 1$ and $f(z) = \sin(1/z)/z$.

This mathematical property applies in many domains of physics, particularly in phase transitions. For example, in the Fisher droplet model[30] the number of clusters of size A at temperature T is given by

$$n(s,T) = s^{-\tau} e^{-K(T-T_c)s^\sigma} \tag{16}$$

i.e. by a scaling invariant part $s^{-\tau}$ and a scaling function $f(z)$. Here K is a constant, σ and τ are two critical exponents and T is the critical temperature. We recall that critical phenomena are the phenomena that manifest in the vicinity of the transition point of a second order phase transition. A critical exponent is a number that describes the behaviour of a physical quantity near that critical point. Consider a real and non-negative function $f(x)$ defined in the interval $]0, x_0]$. If the limit

$$\lambda = \lim_{x \to 0+} \frac{\log f(x)}{\log x} \tag{17}$$

exists when x goes to zero on the positive side, then λ is called the critical exponent to be associated with the function $f(x)$. (The definition is extended straightforwardly to the interval $[x_0, 0[$ when $x \to 0^-$). It is important to stress that the shorthanded notation that will be frequently used

$$f(x) \sim x^\lambda,$$

does not imply that

$$f(x) = Ax^\lambda,$$

where A is a constant. (Take for example the function $f(x) = x^\lambda \mid \log x \mid$, that has λ as critical exponent).

3.1 Signals of scaling in fragmentation

We have seen that the scaling *ansatz* for the cluster size distribution

$$n_s \sim s^{-\tau} f(s/s_\xi) \tag{18}$$

apply to geometrical fragmentation (or aggregation) models as well as to rate equations models. In this section we discuss how to test the existence of such scaling property using experimental data from a fragmentation process.

3.1.1 Critical behaviour and critical exponents

First we concentrate on the possible manifestation of a critical behaviour. In infinite systems, near critical points there are clusters of all sizes and the characteristic cluster size diverges in leading order usually with a power law behaviour

$$s_\xi(x) \sim \mid x - x_c \mid^{-1/\sigma}$$

Then $n_s(x_c) \sim s^{-\tau}$ and $f(o) = 1$. Here x_c is the critical value of the variable x that defines the physical state of the system. For example, in percolation theory $x \equiv p$ (see Eq. 7. For this value x_c the cluster size distribution n_s is singular because all moments m_k with $k > \tau - 1$ diverge. This is shown [11] by

$$m_k(\epsilon) = \sum s^k n_s(\epsilon) \simeq \int_0^\infty s^{k-\tau} F(\epsilon s^\sigma) ds.$$

Or

$$m_k(\epsilon) = \mid \epsilon \mid^{(\tau-k-1)/\sigma} / \sigma \int_0^{\pm\infty} \mid z \mid^{(1+k-\tau)/\sigma} z^{-1} F(z) dz = C^\pm \mid \epsilon \mid^{(\tau-k-1)/\sigma} \tag{19}$$

where we have introduced the variables $\epsilon \equiv x - x_c$, $z = \epsilon s^\sigma$, made the change of function $F(z) = f(z^{1/\sigma})$ and replaced the sum by an integral. Notice that for $p > p_c$ the integral runs from 0 to ∞ and from 0 to $-\infty$ for $p < p_c$. $C^\pm$ are the corresponding values of these integrals. The exponents of the moments $k = 0, 1$ and 2 are called $2 - \alpha, \beta$ and $-\gamma$ respectively, in analogy with thermal critical exponents. Then exponent relations like

$$\gamma + 2\beta = 2 - \alpha = (\tau - 1)/\sigma \tag{20}$$

are automatically fulfilled.

3.1.2 Finite Size Scaling

The above considerations strictly apply to infinite systems. In finite systems, Monte-Carlo simulations show that a fingerprint of a transition remains, but spread out in a finite region around p_c.

For example, the behaviour of Eq. 18 is illustrated in Fig. 2 for the bond percolation model in a cubic lattice. Figures 1*a* and 1*d* show the cluster size distribution far below and above the critical point respectively. We remark that in both situations the distribution of light fragments is a very fast (exponential-like) decreasing function. In addition, above the critical point it exists a distribution of large clusters (centered in this example around $s = 55$) which is not accounted by Eq. 18. Right at the critical point (Fig. 1*b*) the distribution is a power law (remark the change to a log-log plot). Slightly above the critical point (Fig. 1c) one sees the rise of the large cluster at $s = 35$. This behaviour is quite general. Analogous distributions appear in thermal phase transitions and in kinetic processes of cluster formation .

How do the fragment size distribution $n(s)$ and related quantities behave near the critical point as a function of the size S of the fragmenting system ? One predicts[11] a finite size scaling of the type

$$n(s, S) \sim S^{-x} g(s/S^x), \tag{21}$$

where x is a new exponent and g a scaling function. The size s_{max} of the largest fragment produced at the critical point scales as

$$s_{max} \sim S^x \tag{22}$$

In the framework of a geometric picture of cluster production the exponent x is the ratio

$$x = D_f/d$$

of the "fractal dimension" D_f of the clusters to the euclidean dimension d of the physical space. Here the "fractal dimension" is defined through the relation between the mass s and the radius R[3] of the clusters,

$$s \sim R^{D_f}$$

which does not necessarily imply selfsimilarity. A "fractal" is an object with $D \neq d$. In dimension $d = 3$ percolation theory predicts $D_f = 2.5$ at the critical point. Far below the critical point, where only very small fragments are present $D_f = 2$. Far above, the largest fragment is obviously a compact object with $D_f = 3$. Different values of D_f are obtained in other fragment production mechanisms. The fractal dimension can be used to sign the fragmentation process. Following these lines, analysis of experimental data can be found in Refs[37] and [36].

4 Critical behaviour in Nuclear Fragmentation

The first worry one encounters when applying the concepts of critical phenomena to atomic nuclei is how to specify the control parameter ϵ. In principle, looking

[3] R is the typical size of any compact object enclosing the clusters.

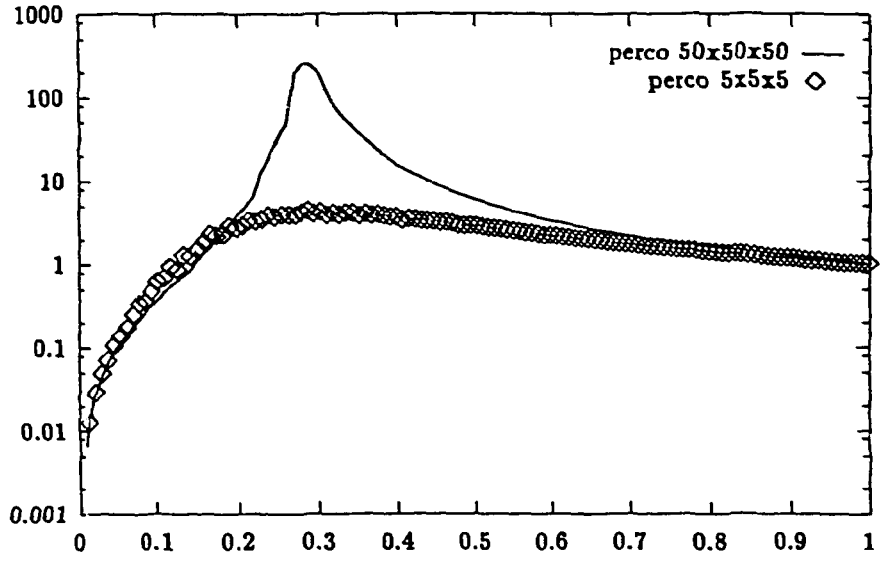

Figure 6: *Mean value of m_2/S as function of m_0/S for small ($S = 125$) and large ($S = 125000$) percolation systems.*

for a thermal phenomenon one would like to choose $\epsilon = T - T_c$, but unfortunately this information is not directly available from experiment. When looking for a "geometrical" phenomenon, like a in percolation fragmentation, one would took $\epsilon = p - p_c$, where p is the bond activation probability and p_c its critical value, but this quantity is even more inaccessible experimentally. One possible solution is to substitute the temperature (or p) by another quantity that is measurable and that is strongly correlated with it. Furthermore, if this correlation is *strictly linear* in the critical region, (this is the case of the control parameter p and the moment m_0 in percolation theory[33]) then taking $\epsilon = m_0 - m_{0crit}$ one can determine directly the correct values of the critical exponents. In thermal phase transitions, the relation between the temperature T and the multiplicity m_0 (or other control parameter) has to be carefully studied. We will discuss below a method that overcomes this difficulty.

The second and more serious difficulty concerns the finite size of atomic nuclei. Strictly speaking, we cannot talk about critical behaviour in a finite size system because none of the moments m_k can diverge. Nevertheless, some aspects of this behaviour remain valid. The critical point is replaced by a "critical region", the width of which increases when decreasing the system size. In the middle of this region, finite and infinite systems behave very differently, but on both sides, these differences are much smaller. Hence it is in principle still possible to extract some information on the exponents by looking at these two regions, but avoiding the central one. This is shown in Fig. 6, where the quan-

	τ	β	γ	$1+\beta/\gamma$
Percolation	2.20	0.45	1.76	1.25
Lattice-gas	2.21	0.33	1.24	1.27
Statis. Equil.	~ 2.2	-	-	2.63 ± 0.07
Au + emul.	2.17 ± 0.1	-	-	1.2 ± 0.1
Au + C	2.14 ± 0.06	0.29 ± 0.2	1.4 ± 0.1	1.21 ± 0.1

Table 2: *Critical exponents for various systems. From refs : Percolation [11],Lattice-gas[35], Statistical Equilibrium Model[36], experimental data on 1 GeV/u Au fragmentation in emulsion [31] and in Au + C reactions[42].*

tity m_2/S is plotted as a function of the control parameter m_0/S for a large percolation cubic lattice and for a small one of the typical size of a nucleus. The similarity is even stronger for the quantity $(S - m_1)/S = < s_{max} > /S$ which plays the role of the "order parameter" in percolation-like theories. In infinite systems, this quantity is finite in the "percolating" phase and zero in the other. We see in Fig. 7 that for $m_0 \ll m_{0crit}$ small and large systems behave similarly but very differently elsewhere.

These two examples give an idea of the difficulties to extract accurate values for the exponents β and γ in nuclear fragmentation. The members of the EOS Collaboration[42] have tried to extract these exponents from their data on 1 GeV/nucleon *Au* projectiles fragmentation. The control parameter is the multiplicity m_0. The critical multiplicity is determined by looking at the best linearity of the curve $\ln < s_{max} >$ for $m_0 < m_{0crit}$ (see Fig. 8) and at the best linearity and best parallelism of the two branches of m_2 (see Fig. 9). These curves are drawn as a function of $ln \mid m_0 - m_{0crit} \mid$. The slopes β and γ are rather sensitive to the choice of m_{0crit}.

In an earlier work[31], the ratio of the exponents β/γ was determined more directly. Representing $\ln < s_{max} >$ versus $ln(m_2/m_1)$ for events of the same type (say, same m_0) one obtains a two-branch curve, the crossing point corresponding to the "critical point" (see Fig. 10). The slope of the lower branch is $1 + \beta/\gamma$. The advantage of this method is that there is no need to fix m_{0crit} and no need for a linear relation between T or p and m_0. The price one pays is that only the ratio of the exponents is measured. Using the data of Waddington and Freier[43] on *Au* fragmentation in emulsion, it was concluded that this ratio is compatible with both percolation and liquid-gas predictions.

The exponent τ is in principle easier to determine, by using Eq. 18 right at the "critical point". The problem is again to define this "point". Here it is also possible to avoid this difficulty, by looking at the slope of $\log m_3/m_1$ versus $\log m_2/m_1$ [31]. Unfortunately, most theories predict very similar values for τ. In any case, one always gets $\tau > 2$ from experiments in nuclear fragmentation.

In Table 2 we synthesize our present knowledge of critical exponents.

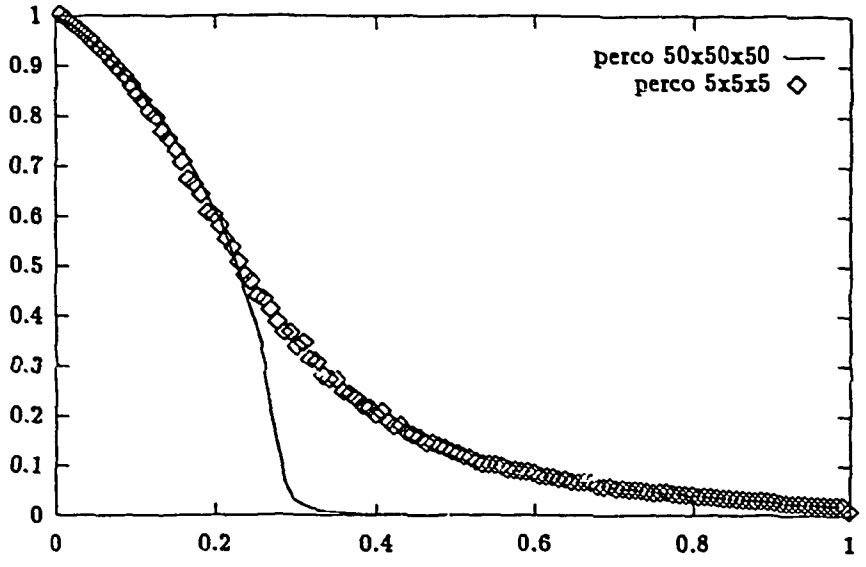

Figure 7: *Mean value of the largest fragment,* $< s_{max} > /S$ *as function of* m_0/S *for small* ($S = 125$) *and large* ($S = 125000$) *percolation systems.*

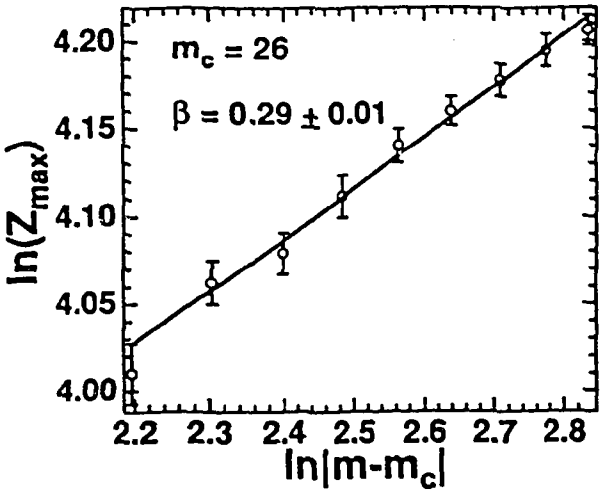

Figure 8: *Example of the determination of the critical exponent* β *for a particular choice of* m_{0crit}. *From Ref. [42].*

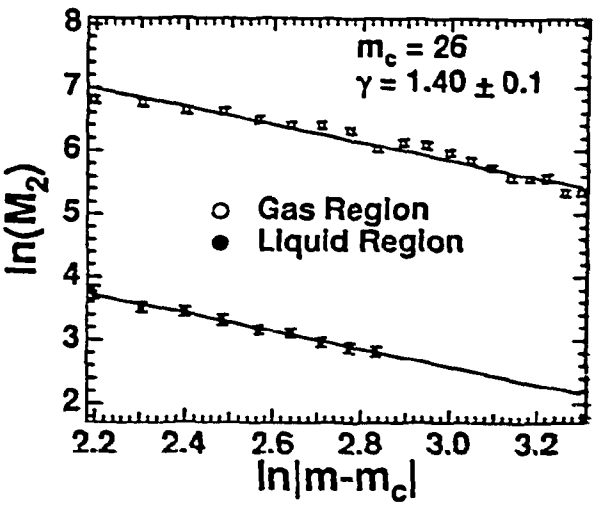

Figure 9: *Example of the determination of the critical exponent γ for a particular choice of m_{0crit}. Liquid and gas regions indicate $m_0 < m_{0crit}$ and $m_0 > m_{0crit}$ respectively. From Ref. [42].*

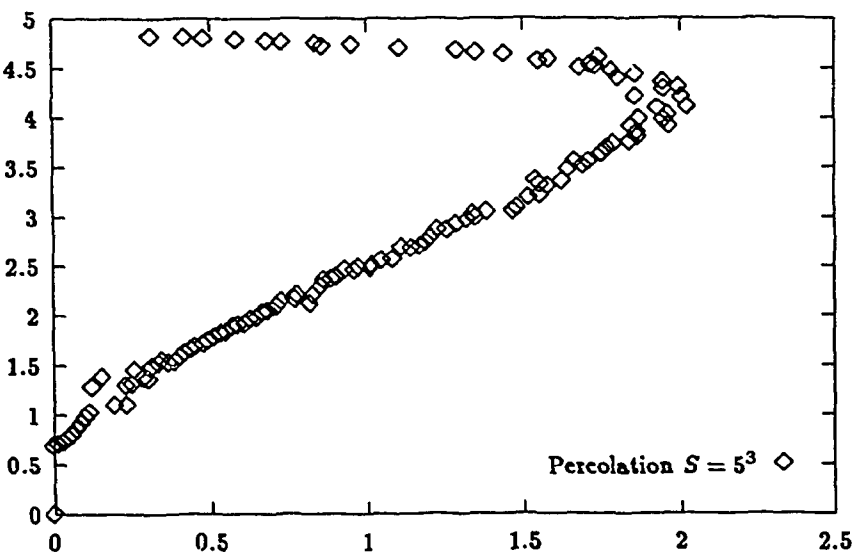

Figure 10: *Size of the largest fragment averaged at fixed multiplicity versus m_2/m_1 on a Log-Log plot.*

We see that the two experimental determinations of β/γ [31, 42] are in good agreement with both liquid-gas and percolation predictions. When determined separately by the EOS collaboration [42] β and γ are in better agreement with the former prediction.

Also shown in Table 2 is the value of β/γ calculated with the statistical equilibrium model[36]. It differs from the two independent *experimental* determinations by a factor of two. This discrepancy deserves further theoretical considerations.

5 Concluding remarks

This Contribution is a short review of the methods to study phase transitions in the fragmentation of finite nuclei. The determination of a set of critical exponents associated to the mean fragment size distribution appears to be the unique way to achieve a definite classification of the transition. This program seems in principle realizable with the new generation of 4π charged particles detectors. However we will temperate this optimism with a few warnings concerning the analysis of experimental data.

We assumed implicitly in the preceeding discussions that the size S of the fragmenting system was invariant. This is not always the case in nuclear fragmentation. At high bombarding energies intermediate mass fragments (the ones that determine mostly the critical behaviour) come from a "spectator" source, which size may change drastically with impact parameter. For example, in ALADIN experiments[34] on 600 MeV/nucleon Au projectiles bombarding Cu targets, for the most violent collisions that have been detected (lowest Z_{bound}) the emitting "spectator" source has on average the size of a Fe nucleus[45]. The influence of this variation of S on the critical exponents should be carefully studied.

At lower bombarding energies (less then 100 MeV/nucleon) we have the problems of the number and the size of emitting sources. As a function of the impact parameter, the reaction mechanism varies from deep inelastic, quasi-fusion and (maybe) total fusion. Even with a complete identification of the fragment momenta it is not possible to determine, event by event, the source of each fragment. This raises various difficulties. What is the multiplicity (or another control parameter) of each source ? What is the largest fragment s_{max} of each source ? (we recall that the subtraction of the largest fragment, at least in the "liquid" or "percolating" phase, is essential to calculate correctly the critical exponents). All these questions deserve a close examination.

References

[1] B. Jakobson et al., *Z. Phys.* **A307** (1982) 293.

[2] L.P. Csernai and J.I. Kapusta, *Phys. Rep.* **131** (1986) 223.

[3] J. Huefner, *Phys. Rep.* **125** (1985) 129.

[4] D.H.E. Gross, *Rep. Prog. Phys.* **53** (1990) 605.

[5] L.G. Moretto and G.J. Wozniak, *Annu. Rev. Nucl. Part. Sci.* **43** (1993) 379.

[6] A. Abramowitz and I.A. Stegun *Handbook of Mathematical Functions* (Dover Inc., New York, N.Y.,1965).

[7] A.J. Cole et al., *Phys. Rev.* **C39** (1989) 891.

[8] J. Aichelin, J. Hüfner and R. Ibarra, *Phys. Rev.* **C30** (1984) 107.

[9] L.G. Moretto and D.R. Bowman, *XXIV Inter. Winter Meeting of Nucl. Phys.* Bormio. Italy. Ricerca Scientifica ed Educazione Permanente (1986) p. 126.

[10] D. Stauffer, A. Coniglio and M. Adam, *Adv. in Pol. Science* **44**(1982) 103.

[11] D. Stauffer, *Introduction to Percolation Theory* (Taylor and Francis Ed., London and Philadelphia, 1985).

[12] L. Landau and E.M. Lifshitz, *Course of theoretical Physics* Vol. 5, Pergamon Press, 1986.

[13] D. Stauffer and C. Jayaprakash, *Phys. Lett.* **A64** (1977) 433.

[14] X. Campi, J. Desbois and E. Lipparini, *Phys. Lett.* **B142** (1984) 8.

[15] W. Bauer et al., *Phys. Lett.***B150** (1985) 536.

[16] X. Campi and J. Desbois, *GSI Report 85-10; XXIII Int. Winter Conf.* , Bormio, Italy. Ricerca Scientifica ed. Educazione Permanente (1985) p. 498.

[17] J. Desbois, *Nucl. Phys.* **A466** (1987) 724.

[18] C. Ngo et al., *Nucl. Phys.* **A499** (1989) 148.

[19] J. Cugnon and C. Volant, *Z. Phys.* **A334** (1989) 435.

[20] S. Leray et al., *Nucl. Phys.* **A531** (1991) 177.

[21] X.Z. Zhang et al., *Nucl. Phys.* **A461** (1987) 641 and references therein.

[22] J. Randrup and S.E. Koonin *Nucl. Phys.* **A356** (1981) 223.

[23] D.H.E. Gross, *Phys. Scr.* **T5** (1983) 213.

[24] A.S. Botvina et al., *Nucl. Phys.* **A475** (1987) 663.

[25] D.H.E. Gross, Yu-Ming Zheng and H. Massmann, *Phys. Lett.* **B200** (1988) 397.

[26] Z. Cheng and S. Redner, *Phys. Rev. Lett.* **58** (1988) 2450.

[27] E.D. McGrady and R.M. Ziff, *Phys. Rev. Lett.* **58** (1987) 892.

[28] R.M. Ziff and E.D. McGrady, *Macromolecules* **19** (1986) 2513.

[29] H.E. Stanley, *Introduction to Phase Transitions and Critical Phenomena* (Clarendon Press, Oxford, 1971).

[30] M.E. Fisher, *Physics* (N.Y.) **3** (1967) 255; *Rep. Prog. Phys* **30** (1967) 615.

[31] X. Campi, *J.Phys. A: Math. Gen.* **19** (1986) L917.

[32] X. Campi, *Phys. Let.* **B208** (1988) 351.

[33] X. Campi and H. Krivine, *Z. Phys.* **A344** (1992) 81.

[34] P. Kreutz et al., *Nucl. Phys.* **A556** (1993) 672.

[35] J.J. Binney, N.J. Dowtick, A.J. Fisher and M.E.J. Newman, *The Theory of Critical Phenomena,* Clarendon Press, Oxford (1992).

[36] H.R. Jaqaman and D.H.E. Gross, *Nucl. Phys.* **A524** (1991) 321.

[37] X. Campi, *Nucl. Phys.* **A495** (1989) 259c.

[38] J.P. Bondorf et al., *Nucl. Phys.* **A443** (1985)321.

[39] Bao-An Li, A.R. DeAngelis and D.H.E. Gross, *Phys. Lett* **B303** (1993) 225.

[40] R.J. Charity et al., *Nucl. Phys.* **A483** (1988) 371.

[41] C. Barbagallo, J. Richert and P. Wagner, *Z. Phys.* **A324** (1986) 97.

[42] A.S. Hirsch et al., To be published in *Phys. Rev. Lett.*

[43] C.J. Waddington and P.S. Freier, *Phys. Rev.* **C31** (1985) 888.

[44] A.S. Hirsch et al., Contribution to the Heavy Ion Conference at LBL, October 1993.

[45] X. Campi, H. Krivine and E. Plagnol, *Phys. Rev. C,* in press.